Review

An Overview of the Behavior of Concentrates with Arsenic, Antimony, and Bismuth under Roasting Conditions

Alvaro Aracena [1,*], Miguel Véliz [1], Oscar Jerez [2], Eduardo Balladares [3] and Manuel Pérez-Tello [4]

[1] Escuela de Ingeniería Química, Pontificia Universidad Católica de Valparaíso,
    Valparaíso 2362854, Chile; miguel.veliz.t@mail.pucv.cl
[2] Instituto de Geología Económica Aplicada, Universidad de Concepción, Concepción 4070386, Chile;
    ojerez@udec.cl
[3] Departamento de Ingeniería Metalúrgica, Facultad de Ingeniería, Universidad de Concepción,
    Concepción 4070386, Chile; eballada@udec.cl
[4] Departamento de Ingeniería Química y Metalurgia, Universidad de Sonora, Hermosillo 83000, Mexico;
    manuel.perez@unison.mx
* Correspondence: alvaro.aracena@pucv.cl

Abstract: It is well-known that the mining industry in Chile and the world is searching for eco-friendly, highly efficient mineral treatments. This is because the content of toxic elements such as arsenic, antimony, and bismuth have increased in the copper concentrates in the last years. This trend has affected the market of this metal, as well as increased the potential of producing solid wastes that represent a threat to the environment. In this paper, a review on the fundamentals of the current treatments aimed at removing arsenic, antimony, and bismuth from copper concentrates under roasting conditions is presented. The literature survey included the research conducted from 2000 until now and is focused on the different types of roasting of copper concentrates reported in the literature. A summary of the experimental conditions and major findings of each work is discussed. Depending on the type of roasting, the behavior of arsenic, antimony, and bismuth species during the experiments is analyzed.

Keywords: arsenic; antimony; bismuth; roasting; pyrometallurgy; volatilization; encapsulation; capture

1. Introduction

Copper concentrates are currently treated by pyrometallurgy routes to obtain intermediate products with a high content of copper. Typical processes include smelting and converting to produce matte and blister copper in molten state. Although such technologies are widely used worldwide, a number of difficulties typically arise during operation. This includes the production of solid and gaseous wastes, which are potentially harmful to the environment, the high costs of energy associated with the operation of high temperature reactors, and the handling of molten materials, among others. Typical copper concentrates obtained by flotation techniques contain chalcopyrite ($CuFeS_2$), bornite (Cu_5FeS_4), and chalcocite (Cu_2S) as major phases. Such concentrates are generally treated by means of high-temperature technologies [1].

The chemical composition of copper concentrates in Chile varies depending on the region where it is obtained. As an example, Table 1 shows a comparison of typical compositions of concentrates from Chuquicamata [2] and of copper sulfide minerals in Northern Chile [3]. The former represented about 5% of the total Chilean copper production in 2022 [2]. Table 1 shows that the chemical composition is strongly dependent upon the region from which the material was obtained.

Figure 1 shows the typical pyrometallurgical route followed by Chilean copper smelters to produce cathodic copper [4,5]. Here, emphasis is made on the compositions of copper, arsenic, antimony, and bismuth in the several products and effluents obtained

during the stages of roasting, smelting, converting, anode casting, and electrowinning. The information shown in Figure 1 is based on plant data collected at the Chuquicamata mine by Barros et al. [3]. It shows that the contents of arsenic, antimony, and bismuth in such streams are significant and, thus, deserve further analysis.

Table 1. Chemical composition of Chuquicamata copper concentrate and copper sulfide minerals in Chile [3], wt%.

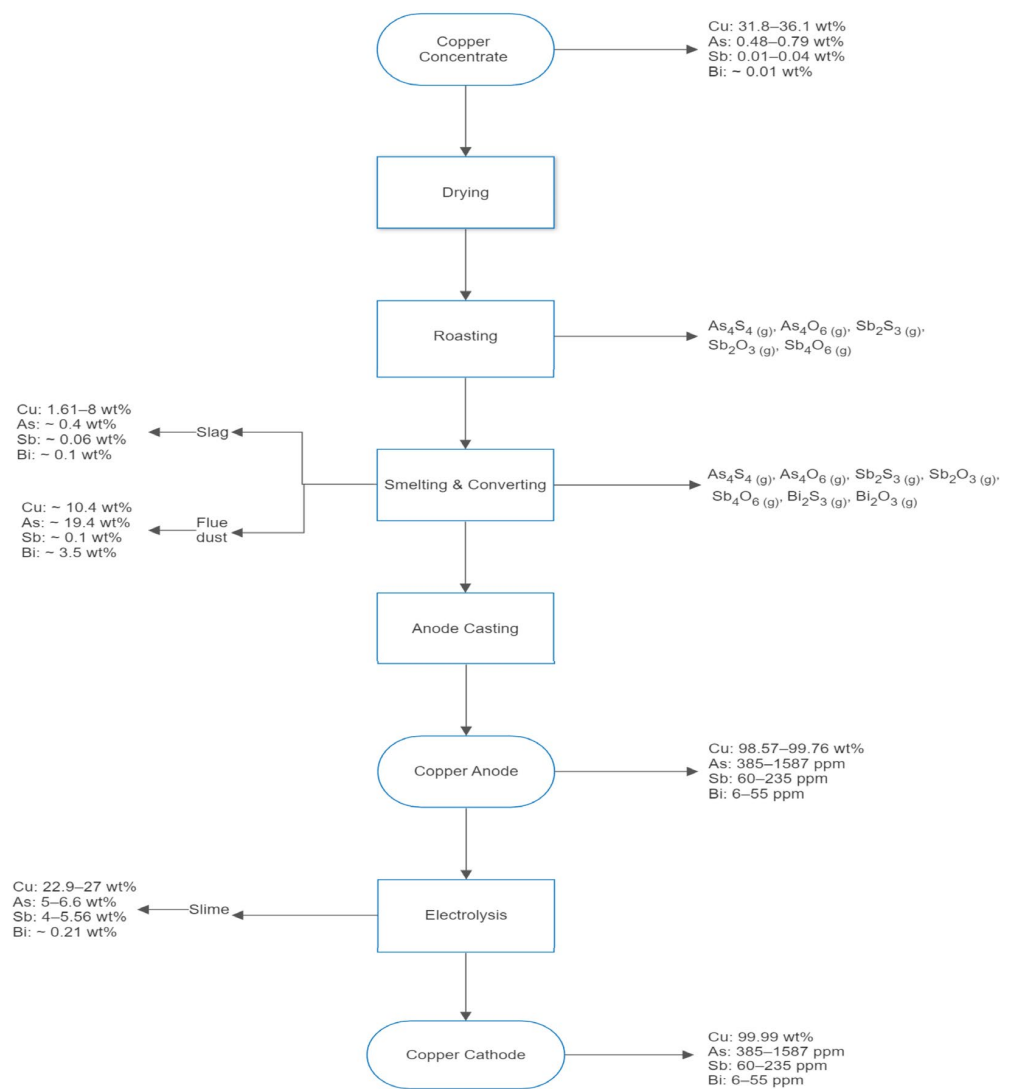| Mine/Region	Chuquicamata Concentrate	Northern Chile Sulfide Minerals
Element		
Cu	31.8–33.5	1.49
As	0.48–0.79	<0.1
Sb	0.012–0.042	-
Bi	0.0069–0.011	-

Figure 1. Flowchart of the copper production from copper concentrate showing the concentration ranges of copper, arsenic, antimony, and bismuth in the main Chilean process and the gaseous products form on roasting and smelting/converting. Data provided by Barros et al. [3].

Arsenic is usually present as enargite (Cu_3AsS_4) and tennantite ($Cu_{12}As_4S_{13}$) [6]; antimony is mostly present as stibnite (Sb_2S_3) and bismuth may be found as elemental bismuth (Bi) or bismuthine (Bi_2S_3). These sulfides are difficult to separate by flotation, especially enargite and tennantite. This is because the physicochemical properties of the Cu–As–S sulfides are similar to other copper sulfides present in the concentrate [7]. As a result, such species are carried towards the smelting and converting steps, where they undergo oxidation at high temperatures and distribute in both gas and molten products. The presence of such elements strongly affects the quality of the copper products, causes contamination of the flue dust, and makes further treatment difficult. It also causes operation problems in the acid plant, the collection of wastes, and decreases the efficiency of the electrorefining cells [8–10].

The lack of control on the rate of volatilization of arsenic, antimony, and bismuth species during the processing of copper concentrates may cause serious health problems in the human population and represent a threat to living beings in general. An example of the toxicity of these species is the use of diphenylchloroarsine ("adamsite"), a compound composed of arsenic and chloride used as a chemical weapon in World War I [11].

At the present time, few reviews on the pyrometallurgical processing of copper concentrates with high contents of arsenic, antimony, and bismuth are available in the literature. The latest work on the processing of arsenic species was reported by Castro et al. [12], who analyzed the behavior of arsenic sulfides at high temperatures. Regarding the processing of antimony, Moosavi et al. [13] carried out a review on its development through history. The authors focused on the pyrometallurgical route as well as the technologies used to obtain antimony-based products. Compared to arsenic and antimony, the literature on the processing of bismuth is scarce. The present paper is aimed at reviewing the current information on the subject. Such information is provided in a concise, compact form so that the interested reader may find it quickly in the form of tables.

2. Literature Review

Recent studies show that enargite begin oxidation at 375 °C producing tennantite ($Cu_{12}As_4S_{13}$) and sulfur dioxide (SO_2) according to Reaction (1):

$$4\, Cu_3AsS_{4\,(s)} + 3\, O_{2\,(g)} = Cu_{12}As_4S_{13\,(s)} + 3\, SO_{2\,(g)} \tag{1}$$
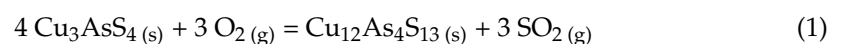
Both decomposition and oxidation rates of enargite were observed to be strongly dependent upon temperature and oxygen concentration. Further oxidation of tennantite produced gaseous As_4O_6 according to Reaction (2) [14]:

$$Cu_{12}As_4S_{13\,(s)} + 10\, O_{2\,(g)} = 6\, Cu_2S_{\,(s)} + As_4O_{6\,(g)} + 7\, SO_{2\,(g)} \tag{2}$$
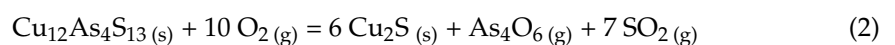
These studies updated reaction mechanisms of tennantite proposed by Secco et al. [15], whose results had similar behavior to the work done by Yoshimura [16]. Padilla et al. [14] showed that under the presence of gaseous oxygen, enargite (Cu_3AsS_4) first oxidizes at 375 °C producing tennantite ($Cu_{12}As_4S_{13}$) and sulfur dioxide gas (SO_2), then tennantite further oxidizes according to Reaction (2).

Under neutral roasting conditions, enargite is assumed to undergo thermal decomposition to produce gaseous As_2S_3 as the major arsenic gaseous species according to Reaction (3) [15,16].

$$2\, Cu_3AsS_{4\,(s)} = 3\, Cu_2S_{\,(s)} + As_2S_{3\,(g)} + S_{2\,(g)} \tag{3}$$
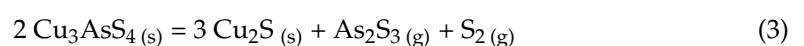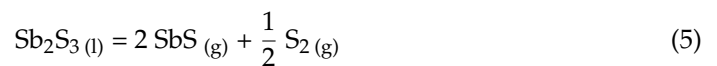
In a further study, Padilla et al. [17] used a thermogravimetric analysis technique to conclude that the thermal decomposition of enargite produces As_4S_4, as shown in Reaction (4).

$$4\, Cu_3AsS_{4\,(s)} = 6\, Cu_2S_{\,(s)} + As_4S_{4\,(g)} + 3\, S_{2\,(g)} \tag{4}$$
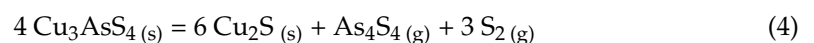
Regarding the behavior of antimony, this element is mostly removed in the off-gas streams of smelting and converting processes [18]. This is because antimony and its oxides are volatile at the typical temperatures under which such processes operate. Despite such behavior, during industrial operation, a significant portion of antimony is retained in the condensed phases [18–20]. Furthermore, the elucidation of the mechanisms of the decomposition of stibnite (Sb_2S_3) is relevant for the control of antimony content in both the calcine and condensed phases. It may also help to explain its distribution in subsequent stages of the production process.

Reactions (5) through (7) have been proposed for the decomposition of antimony trisulfide in molten state in a neutral atmosphere.

$$Sb_2S_{3\,(l)} = 2\,SbS_{(g)} + \frac{1}{2}\,S_{2\,(g)} \tag{5}$$

$$Sb_2S_{3\,(l)} = 2\,Sb_{(l)} + 3/2\,S_{2\,(g)} \tag{6}$$

$$Sb_2S_{3\,(l)} = Sb_2S_{3\,(g)} \tag{7}$$

Reactions (5)–(7) were reported by Faure et al. [21], Shendiyapin et al. [22], and Komorova et al. [23], respectively. Reaction (5) indicates that molten Sb_2S_3 decomposes into antimony sulfide gas and sulfur gas; Reaction (6) states that decomposition occurs with the formation of metallic antimony, whereas Reaction (7) represents the volatilization of molten Sb_2S_3 as a physical process in which the molecular structure is conserved. The dominant step in the above set of reactions depends on the temperature of operation. Reaction (5) prevails in the range of 670 and 793 K, whereas Reaction (6) prevails between 873 and 1097 K. Finally, Reaction (7) predominates at temperatures higher than 1097 K.

Under the presence of gaseous oxygen, Sb_2S_3 is rapidly oxidized to produce valentinite (Sb_2O_3) [24,25]. These authors proposed that stibnite is oxidized to valentinite and, in a consecutive step, it is over-oxidized to antimony dioxide or cervantite (SbO_2).

On the other hand, most bismuth sulfides are commonly found in association with lead, copper, and silver. Some bismuth phases found in ore deposits include bismuthine (Bi_2S_3), bismite (Bi_2O_3), and bismuth ochre ($Bi_2O_3 \cdot 3H_2O$).

Bismuth is found mainly around intrusive rocks, so it is paramagnetic. Bismuthine is the impurity usually found in chalcopyrite-based copper concentrates. Part of the bismuthine present in the concentrates is eliminated in the gas phase during the pyrometallurgical processes [26]. Furthermore, it was reported that 30 to 75% of bismuth in the concentrate is distributed in the matte phase, 5 to 30% in the slag phase, and 15 to 65% in the gas phase during the smelting operation [27].

It is of interest to note that of all three elements of study (As, Sb and Bi), bismuth is the element with the fewest studies reported in the literature since 2000. Furthermore, the information on the processing of bismuth species is scarce.

In this paper, any chemical species containing arsenic, antimony, and bismuth in its structure is considered as a toxic compound. According to the operating conditions under which such compounds are treated, the processes may be classified into three groups: thermal decomposition or inert roasting, oxidative roasting, and reductive roasting. The choice of the type of roasting to be used to treat a specific compound depends on the goal to be achieved; namely, the volatilization of the toxic compound for further cleaning of the carrying gas stream, or the capture of the toxic compound by a solid phase for a nonvolatile post-treatment.

2.1. Thermal Decomposition or Inert Roasting

In general, the concentrates containing As, Sb, and Bi are treated by roasting in a neutral environment (nitrogen, argon, etc.), which causes the volatilization of these elements. Inert roasting can achieve high efficiency removal, but the nature of the products

and removal efficiency vary with the temperature of operation. As an example, the roasting of antimony trisulfide (Sb_2S_3) in the range of 973–1123 K proceeds according to Reaction (7) [28,29]. However, at temperatures higher than 1123 K, Reactions (5) and (6) occur simultaneously. Further, the metallic antimony produced by Reaction (6) slowly volatilizes as a result of its low equilibrium partial pressure:

$$Sb_{(l)} = Sb_{(g)} \tag{8}$$

This phenomenon was also observed with antimony (III) oxide (Sb_2O_3). Under a neutral environment and below 1273 K, such species volatilizes according to reaction (9) [29,30].

$$2\,Sb_2O_{3\,(l)} = Sb_4O_{6\,(g)} \tag{9}$$

At temperatures higher than 1273 K, thermal decomposition produces a variety of both volatile and non-volatile compounds [28,31].

$$Sb_2O_{3\,(l)} = SbO_{2\,(l)} + SbO_{(g)} \tag{10}$$

$$2\,SbO_{2\,(l)} = 2\,SbO_{(g)} + O_{2\,(g)} \tag{11}$$

To test whether a particular species tends to volatilize, the Clausius–Clapeyron equation may be used to calculate its vapor pressure. Table 2 shows the parameters of the Clausius–Clapeyron equation for arsenic [32], antimony [33], antimony trisulfide [34], and bismuth [32]. Figure 2 shows the vapor pressure of elemental arsenic, antimony, and bismuth in the range of 1073–1473 K. As expected, the vapor pressure increases with temperature.

Table 2. Clausius–Clapeyron equation parameters for arsenic, bismuth, and antimony trisulfides, P in Pascals.

Compound/Element *	A	B	Reference
As [1]	−20,689	10.62	[32]
Sb [1]	−28,535	12.336	[33]
Sb_2S_3 [2]	−(10,490 ± 200)	13.96 ± 0.2	[34]
Bi [1]	−21,702	11.75	[32]

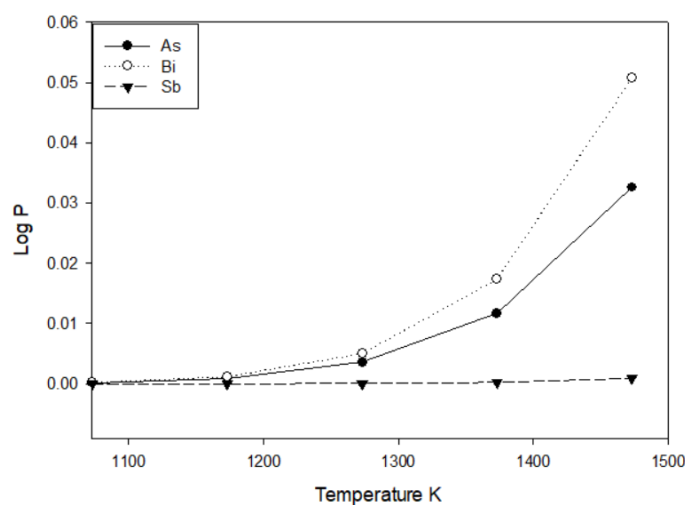* $X^{(1)}$: Log P = exp (A/T + B), $X^{(2)}$: Log P = (A/T + B).

Figure 2. Vapor pressure of elemental arsenic, antimony and bismuth between 1073–1473 K. Pressure in Pascals.

Table 3 shows a summary of the studies on As, Sb, and Bi species of industrial interest. Relevant information regarding the experimental techniques used and the range of temperature under which volatilization was observed are also shown.
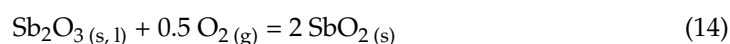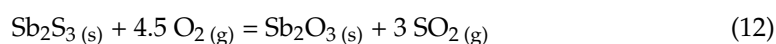
Table 3. Compilation of inert roasting studies of arsenic, antimony, and bismuth species.

Compound	Material *	Experimental Technique *	Volatilization	Reference
Sb_2O_3	M [32], C [35], S [28,30,31]	TG [28,30,31,35], TG/DSC [32]	823–1423 K	[28,30–32,35]
SbO_2	S	TG	>1423 K	[28,31]
Sb_2S_3	S	TG [28,29,31], TG/DSC [36]	973–1423 K	[28,29,31,36]
Sb	S	TG	1223 K	[28,29]
$Cu_{12}Sb_4S_{13}$	M	TG	973–1473 K	[36,37]
Bi_2S_3	C [38], S [39]	TG/DSC [38], TG/MS [39]	No	[38,39]
Bi_2O_3	C	TG/DSC	No	[40]
As_2O_3	C [35,41,42], S [40,43]	TG [40,42], TG/DSC [35,41,43]	623–1273 K	[35,40–43]
Cu_3AsS_4	M [14,44–46], C [17,47,48]	TG [14,44–47], FB [48], TG/DSC [17]	848–1773 K	[14,17,44–48]
$Cu_{12}As_4S_{13}$	M [37,49], C [45,48,50]	TG [37,47,49,50], TG/DTG [48]	848–1773 K	[37,47–50]

* Material: mineral (M), concentrate (C) or synthetic (S) or not apply (NA). Experimental technique: thermogravimetric (TG), fluidized bed (FB), derivative thermogravimetry (DTG), differential scanning calorimetry (DSC), differential thermal analysis (DTA), inductively coupled plasma atomic emission spectroscopy (ICP-AES) or mass spectroscopy (MS), not apply (NA).

2.2. Oxidative Roasting

Unlike inert roasting, under the presence of oxygen, oxidation takes place. Furthermore, oxide species are formed. Oxidation does not necessarily produce volatile species. As an example, the oxidative roasting of antimony trisulfide in the range of 973–1273 K occurs via the following reactions [28].

$$Sb_2S_{3\,(s)} + 4.5\,O_{2\,(g)} = Sb_2O_{3\,(s)} + 3\,SO_{2\,(g)} \tag{12}$$

$$Sb_2O_{3\,(s,\,l)} = Sb_2O_{3\,(g)} \tag{13}$$

$$Sb_2O_{3\,(s,\,l)} + 0.5\,O_{2\,(g)} = 2\,SbO_{2\,(s)} \tag{14}$$

When oxidative roasting is carried out under low oxygen partial pressure (1% to 5%), Sb_2S_3 produces Sb_2O_3 and the sulfur is volatilized as sulfur dioxide gas. Further, Sb_2O_3 undergoes volatilization. Reaction (14) requires a high partial pressure of oxygen to produce antimony dioxide (SbO_2), also known as cervantite. This species begins to volatilize past 1373 K under the following decomposition reaction.

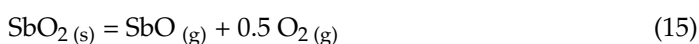$$SbO_{2\,(s)} = SbO_{(g)} + 0.5\,O_{2\,(g)} \tag{15}$$

Table 4 summarizes the corresponding studies on the oxidative roasting of As, Sb, and Bi species of interest for this work.

Table 4. Compilation of oxidative roasting studies of arsenic, antimony, and bismuth species.

Compound	Material *	Reagents	Experimental Technique *	Volatilization	Reference
Sb_2O_3	S	$O_{2 (g)}$	TG	No	[51]
Sb_2S_3	C [52,53], S [28,29]	$O_{2 (g)}$	TG/DSC	No	[28,29,52,53]
Sb	S	$O_{2 (g)}$	TG	No	[29]
$Cu_{12}Sb_4S_{13}$	M	$O_{2 (g)}$	TG	773–1473 K	[37]
Bi_2S_3	M	MnO_2, Mn_2O_3, $O_{2 (g)}$	TG	No	[54]
As_2S_3	C	$O_{2 (g)}$	FB	873–1173 K	[48,55]
As_2O_3	C [56], NA [45]	$Ca(OH)_2$, Fe_2O_3, $O_{2 (g)}$	TG [56], NA [45]	No	[45,56]
As_4O_6	C [41,57], S [40]	CaO, Cu_2O, CuO, Fe_2O_3, $O_{2 (g)}$	TG [40], TG/DSC [41,57]	No	[40,41,57]
Cu_3AsS_4	M	$O_{2 (g)}$	TG	648–898 K	[14,47,58,59]
$Cu_{12}As_4S_{13}$	M [36], C [50]	$O_{2 (g)}$	TG	723–1323 K	[36,50]
FeAsS	C [56,59], NA [45]	$O_{2 (g)}$	TG [56,59], NA [45]	673–1173 K	[45,56,59]
$Cu_3(AsO_4)_2$	NA	FeS_2, $O_{2 (g)}$	NA	>873 K	[60]
$Ca_2As_2O_7$	S	$O_{2 (g)}$	TG	>1223 K	[40]

* Material: mineral (M), concentrate (C), synthetic (S) or not apply (NA). Experimental technique: thermogravimetric (TG), fluidized bed (FB), derivative thermogravimetry (DTG), differential scanning calorimetry (DSC), differential thermal analysis (DTA), inductively coupled plasma atomic emission spectroscopy (ICP-AES) or mass spectroscopy (MS), not apply (NA).
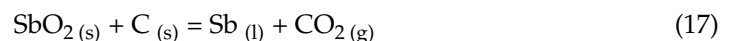
2.3. Reductive Roasting

Reductive roasting is an efficient method to produce non-volatile products in which As, Sb, and Bi are captured. An example is the carbothermal reduction of stibine in which the production of sulfur and Sb in the gas phase is avoided [31,51].

The reduction of Sb_2S_3 using CaO as sulfur carrier between 973–1173 K proceeds according to the following reactions [51]. All the Gibbs free-energy data for the reduction reactions was collected from HSC database [61].

$$2\ Sb_2S_{3\ (s)} + 6\ CaO_{\ (s)} = Sb_{\ (l)} + 3\ SbO_{2\ (s)} + 6\ CaS_{\ (s)} \tag{16}$$

$$\Delta G\ 973\ K = 56.450\ kJ/mol$$

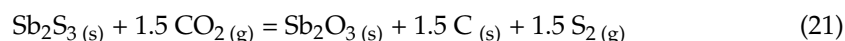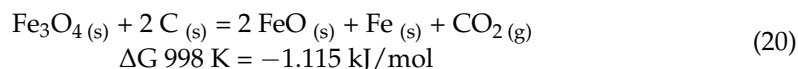$$SbO_{2\ (s)} + C_{\ (s)} = Sb_{\ (l)} + CO_{2\ (g)} \tag{17}$$

$$\Delta G\ 973\ K = -122.634\ kJ/mol$$

Once $CO_{2\ (g)}$ begins to form according to reaction (17), it reacts with carbon to form $CO_{\ (g)}$ (carbon monoxide). Further, CO is consumed according to reaction (19).

$$C_{\ (s)} + CO_{2\ (g)} = 2\ CO_{\ (g)} \tag{18}$$

$$SbO_{2\ (s)} + 2\ CO_{\ (g)} = Sb_{\ (l)} + 2\ CO_{2\ (g)} \tag{19}$$

$$\Delta G\ 998\ K = -122.619\ kJ/mol$$

Reaction (19) is the predominant step, as typically solid–gas reactions, such as Reaction (18), are faster than solid–solid reactions (Reaction (17)). On the other hand, the reduction of stibine using fayalite slag (Fe_3O_4 and Fe_2SiO_4) as sulfur carrier, between 998–1173 K proceeds according to the following reactions [31].

$$Fe_3O_{4\ (s)} + 2\ C_{\ (s)} = 2\ FeO_{\ (s)} + Fe_{\ (s)} + CO_{2\ (g)}$$
$$\Delta G\ 998\ K = -1.115\ kJ/mol \tag{20}$$

$$Sb_2S_{3\ (s)} + 1.5\ CO_{2\ (g)} = Sb_2O_{3\ (s)} + 1.5\ C_{\ (s)} + 1.5\ S_{2\ (g)} \tag{21}$$

$$\Delta G\ 998\ K = 309.573\ kJ/mol$$

In this reaction scheme, magnetite is first reduced with coal according to Reaction (20) to produce wustite (FeO), metallic iron (Fe), and CO_2. In the second step, Sb_2S_3 reacts with CO_2 to produce Sb_2O_3, which is further encapsulated by the remaining magnetite, forming tripuhyite ($FeSb_2O_6$).

$$Sb_2O_{3\ (s)} + 1.5\ Fe_3O_{4\ (s)} = FeSb_2O_{6\ (s)} + 5\ FeO_{\ (s)} \tag{22}$$
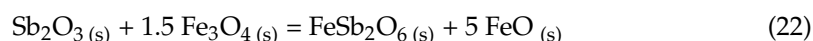
The wustite generated in Reactions (20) and (22) also reacts with senarmontite (Sb_2O_3) to form tripuhyite.

$$Sb_2O_{3\ (s)} + 3\ FeO_{\ (s)} = FeSb_2O_{6\ (s)} + 2\ Fe_{\ (s)} \tag{23}$$
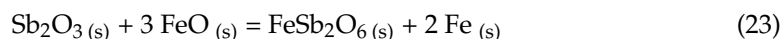
At temperatures higher than 1373 K, part of the senarmontite produced is decomposed to produce antimony oxide gas ($SbO_{\ (g)}$) and cervantite, as shown in Reactions (14) and (15). Table 5 shows a summary of the reductive roasting studies of As, Sb, and Bi species so far reported in the literature.

Table 5. Compilation of reductive roasting studies of arsenic, antimony, and bismuth species.

Compound	Material *	Reagents	Experimental Technique *	Volatilization	Reference
Sb_2O_3	C [52], S [31,62]	Fe, FeO, Fe_2O_3, C, Sb_2S_3	TG	No	[31,52,62]
Sb_2S_3	C [63,64], S [31,36,52,65–67]	C, $CO_{\ (g)}$, CaO, Fe_2O_3, Na_2CO_3, Fe_3O_4, ZnO	TG [31,51,63,64], TG/DSC [36], TG/DTA [65–67]	No	[31,36,51,63–67]
SbO_2	S	C, $CO_{\ (g)}$	TG	No	[28]
$Cu_{12}Sb_4S_{13}$	C	CuO	TG	No	[68]
Bi_2S_3	C [38,68], S [39]	C, $CO_{\ (g)}$, $CO_{2\ (g)}$, Fe_3O_4, Fe_2O_3, FeO	TG/DTG [68], TG/DSC [38], TG/MS [39]	No	[38,39,68]
Bi_2O_3	C [38], S [39]	C, $CO_{\ (g)}$, $CO_{2\ (g)}$, Fe_3O_4, Fe_2O_3	TG/DSC [38], TG/MS [39]	No	[38,39]
As_2O_3	C [41,69,70], S [71]	C, $CuSO_4$, CuS, NaOH, $CaSO_4$	TG [71], TG/DTG [69], TG/DSC [41,70]	No	[41,69–71]
As_2O_5	C	C, $CO_{\ (g)}$, NaOH	TG/DTG [69], TG/DSC [41,70]	No	[41,69,70]

Table 5. *Cont.*

Compound	Material *	Reagents	Experimental Technique *	Volatilization	Reference
$Cu_3(AsO_4)_2$	C	C, H_2SO_4, FeS_2, FeS	TG/DTG [69], TG/DSC [41]	573–823 K	[41,69]
$Na_6As_2O_8$	C	C	ISP/AES [71], TG [72]	873–1073 K	[71,72]
$FeAsO_4$	C	NaOH	TG/DSC	No	[70]
$Bi(AsO_4)$	C	C, $CO_{(g)}$	NA	No	[73]
$Zn_3(AsO_4)_2$	C	C, $CO_{(g)}$	TG	No	[74]
$FeAsO_4$	S	CaO, Fe_2O_3, SiO_2, Na_2CO_3	TG	1273–1523 K	[75]

* Material: mineral (M), concentrate (C) or synthetic (S) or not apply (NA). Experimental technique: thermogravimetric (TG), fluidized bed (FB), derivative thermogravimetry (DTG), differential scanning calorimetry (DSC), differential thermal analysis (DTA), inductively coupled plasma atomic emission spectroscopy (ICP-AES) or mass spectroscopy (MS), not apply (NA).

The overall mechanisms discussed above for neutral, oxidative, and reductive roasting of arsenic, antimony, and bismuth species are schematically summarized in Figure 3. Here, the type of atmosphere, chemical species being processed and produced, the possible outcome regarding the volatilization, and the gaseous products obtained are shown. It is noted that this a general diagram, the details concerning specific data were shown in Tables 3–5.
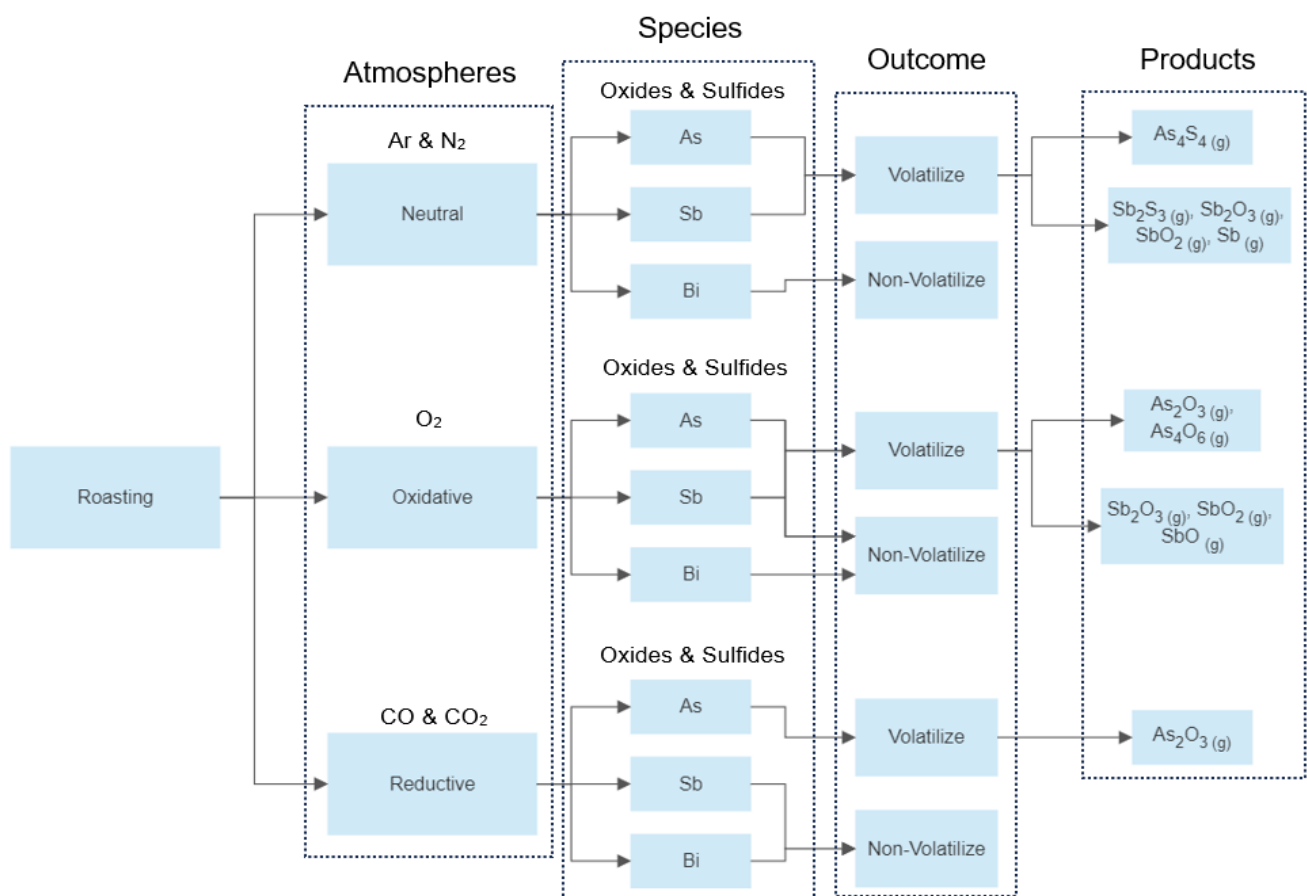

Figure 3. Overall schematic representation of the mechanisms of neutral, oxidative, and reductive roasting of arsenic, antimony, and bismuth species. See Tables 3–5 for details.

3. Discussion

The treatment of a specific compound by inert, oxidative, or reductive roasting does not guarantee the desired result if the experimental conditions are not established from the beginning of the experiment. This is because a number of factors affect the outcome of such experiments, such as the following.

Particle size: Relatively large particles in the treatment of these concentrates can be beneficial to maintain a control in the roasting and reduce the environmental impact. This is because fine particles may be carried away by the off-gas stream [68].

Temperature: The information shown in Table 3 through Table 5 show the temperature ranges under which volatilization and other chemical reactions of the species of interest may occur. Under such conditions, gas phase species, decomposition products, low partial pressure products, or passivating layers may be observed.

Origin of the compound: This is related to the activation energy of the chemical reactions, the reaction rate, the gas flux, and the experimental technique needed to track the evolution of the chemical processes. Based on the previous information, the following discussion addresses the main features of the processes analyzed.

3.1. Antimony

Because this element has a high vapor pressure, it tends to form volatile compounds. Depending on the experimental conditions, a variety of species can be formed.

Under a neutral atmosphere and in the absence of oxygen, antimony species are highly volatile. As an example, solid Sb_2O_3 under neutral atmosphere readily evaporates without passing through a liquid state. In contrast, under presence of gaseous oxygen SbO_2 or SbO is formed, depending on the oxidizing conditions [51].

Finally, under reductive roasting or carbothermal reduction conditions, the volatilization of antimony species may occur as long as the temperature is high enough to volatilize the compound before it starts reacting with the reducing reactant ($CO_{(g)}$, $CO_{2\,(g)}$). This is especially relevant when a significant amount of antimony is volatilized before the reduction reactions form a stable compound. Other reducing reactants include Fe_2O_3 and FeO to produce stable species such as $FeSb_2O_6$ [31]. This method prevents the compound from escaping the system.

3.2. Arsenic

The behavior of As is similar to that of Sb discussed previously. Under oxidative conditions, arsenic will not volatilize unless the arsenic compound presents a high vapor pressure, which increases with the temperature as shown in Figure 2. Some authors [46,56] used metallic compounds such as Fe_2O_3 and CaO in addition to oxygen to form $FeAsO_4$ and $Ca_3(AsO_4)_2$, thus avoiding the volatilization of arsenic. This guaranteed the stabilization of arsenic in a solid phase.

During carbothermal reduction, solid products are formed, as the goal of such treatment is to capture and stabilize the volatile element by adding metallic compounds or salts, such as FeS, Fe_2O_3, or $NaOH$. It is noted that both arsenic and antimony behave similarly under identical process conditions. An example is the formation of volatile trioxides. The major difference between both elements is the high toxicity of arsenic. Furthermore, for the handling and processing of arsenic species, the safety regulations must be more stringent than those for antimony species. This reduces the risk of escapes to the environment, thus preventing hazards to the natural flora and fauna.

3.3. Bismuth

In contrast with the behavior of As and Sb species discussed previously, bismuth species typically show a low vapor pressure, and thus are mostly nonvolatile. Furthermore, no volatilization was observed in the studies shown in Table 3 through Table 5 under a variety of experimental conditions. As an example, Bi_2S_3 under a neutral atmosphere decomposes to form metallic bismuth (Bi) and gaseous sulfur at temperatures lower than

1773 K. Under oxidative roasting conditions, Bi_2S_3 tends to oxidize to form Bi_2O_3 and SO_2 gas. Finally, under carbothermic reduction conditions with addition of Fe_2O_3 and Na_2O_3, the products are metallic bismuth (Bi), the sulfur species FeS and Na_2S, and gaseous CO_2.

4. Conclusions

A survey of the literature was conducted to summarize the characteristics of inert, oxidative, and reducing roasting to process copper concentrates with significant contents of As, Sb, and Bi.

It was shown that the selection of the type of roasting to be used depends on the goal to be achieved; namely, the separation of the metals of interest in the form of a variety of volatile species, or its capture in a solid phase for further disposal. For the former, inert and oxidative roasting may be used, whereas for the latter, reduction roasting is most appropriate. Of all three elements considered in this review, Bi was observed not to produce gaseous products under typical roasting conditions.

Because the chemistry of all three elements is complex, the selection of the experimental conditions to treat a particular material must be done with caution. This is because the products vary substantially with temperature, type of reactants, and processing time. Finally, both theoretical and experimental research are needed to further elucidate the mechanisms governing the chemistry of As, Sb, and Bi species at high temperatures.

References

1. Dimitrijević, M.; Kostov, A.; Tasić, V.; Milosević, N. Influence of Pyrometallurgical Copper Production on the Environment. *J. Hazard. Mater.* **2009**, *164*, 892–899. [CrossRef] [PubMed]
2. COCHILCO Producción Minera. Available online: https://www.cochilco.cl/Paginas/Estadisticas/Bases%20de%20Datos/Producci%C3%B3n-Minera.aspx (accessed on 28 June 2023).
3. Barros, K.S.; Vielmo, V.S.; Moreno, B.G.; Riveros, G.; Cifuentes, G.; Bernardes, A.M. Chemical Composition Data of the Main Stages of Copper Production from Sulfide Minerals in Chile: A Review to Assist Circular Economy Studies. *Minerals* **2022**, *12*, 205. [CrossRef]
4. Aracena, A.; Fuenzalida, P. *Pirometalurgia: Conceptos y Problemas*; Ediciones Universitarias de la Universidad Catolica de Valparaiso: Valparaiso, Chile, 2021; pp. 161–325.
5. Habashi, F. *Extractive Metallurgy of Copper*; Annika Parance: Montreal, QC, Canada, 2012; pp. 115–140. ISBN 9782922686197.
6. Long, G.; Peng, Y.; Bradshaw, D. A Review of Copper–Arsenic Mineral Removal from Copper Concentrates. *Miner. Eng.* **2012**, *36–38*, 179–186. [CrossRef]
7. Sasaki, K.; Takatsugi, K.; Kaneko, K.; Kozai, N.; Ohnuki, T.; Tuovinen, O.; Hirajima, T. Characterization of Secondary Arsenic-Bearing Precipitates Formed in the Bioleaching of Enargite by Acidithiobacillus Ferrooxidans. *Hydrometallurgy* **2010**, *104*, 424–431. [CrossRef]
8. Riveros, G.; Utigard, T.A. Disposal of Arsenic in Copper Discharge Slags. *J. Hazard. Mater.* **2000**, *77*, 241–252. [CrossRef]
9. Basha, C.A.; Somasundaram, M.; Kannadasan, T.; Lee, C.W. Heavy Metals Removal from Copper Smelting Effluent Using Electrochemical Filter Press Cells. *Chem. Eng. J.* **2011**, *171*, 563–571. [CrossRef]
10. Lane, D.J.; Cook, N.J.; Grano, S.R.; Ehrig, K. Selective Leaching of Penalty Elements from Copper Concentrates: A Review. *Miner. Eng.* **2016**, *98*, 110–121. [CrossRef]
11. Calvo Sevillano, G. *Historia del Arsenico*; Almuzara: Cordoba, Spain, 2021.
12. Castro, K.; Balladares, E.; Jerez, O.; Pérez-Tello, M.; Aracena, Á. Behavior of As/As_xS_y in Neutral and Oxidizing Atmospheres at High Temperatures—An Overview. *Metals* **2022**, *12*, 457. [CrossRef]
13. Moosavi-Khoonsari, E.; Mostaghel, S.; Siegmund, A.; Cloutier, J.P. A Review on Pyrometallurgical Extraction of Antimony from Primary Resources: Current Practices and Evolving Processes. *Processes* **2022**, *10*, 1590. [CrossRef]

14. Padilla, R.; Aracena, A.; Ruiz, M.C. Reaction Mechanism and Kinetics of Enargite Oxidation at Roasting Temperatures. *Metall. Mater. Trans. B* **2012**, *43*, 1119–1126. [CrossRef]

15. Secco, A.C.; Riveros, G.; Lupaschi, A. Thermal Decomposition of Enargite and Phase Relations in the System Cu-As-S; Copper 95, C. Diaz, C. Landolt and A. Lurashi, 1988; Volume 4. Available online: https://scholar.google.com/scholar_lookup?title=Thermal+decomposition+of+enargite+and+phase+relations+in+the+system+copper-arsenic-sulfur&author=Secco,+A.C.&author=Riveros,+G.A.&author=Luraschi,+A.A.&publication_year=1988&pages=225%E2%80%93238 (accessed on 1 June 2023).

16. Yoshimura, Z. Bull. Inst. Min; Metall. JPN, 1962; Volume 75. Available online: https://scholar.google.com/scholar?hl=en&as_sdt=0%2C5&q=The+Fundamental+Investigation+of+De-arsenising+Roasting+of+Copper+Concentrates+and+its+Industrial+Practices&btnG= (accessed on 1 June 2023).

17. Padilla, R.; Fan, Y.; Wilkomirsky, I. Decomposition of Enargite in Nitrogen Atmosphere. *Can. Metall. Q.* **2001**, *40*, 335–342. [CrossRef]

18. Davenport, W.G.; King, M.J.; Schlesinger, M.; Biswas, A.K.; Sole, K.C. *Extractive Metallurgy of Copper*; Pergamon Press: Londres, Inglaterra, 2002.

19. Sohn, H.S.; Fukunaka, Y.; Oishi, T.; Sohn, H.Y.; Asaki, Z. Kinetics of As, Sb, Bi and Pb Volatilization from Industrial Copper Matte during Ar+O2 Bubbling. *Metall. Mater. Trans. B* **2004**, *35*, 651–661. [CrossRef]

20. Arias Arce, V.; Coronado Falcón, R.; Puente Santibañez, L.; Lovera Dávila, D. Refractariedad de Concentrados Auriferos. *Rev. Del Inst. De Investig. De La Fac. De Minas Metal. Y Cienc. Geográficas* **2005**, *8*, 5–14.

21. Faure, F.M.; Mitchell, M.J.; Bartlett, R.W. Vapour Pressure Study of Stibnite Sb2S3. *High Tem. Sci.* **1972**, *4*, 181–191.

22. Shendiyapin, A.C.; Nestlerov, U.N.; Ibragimov, E.T. Davlenye Para Trehsernistoy Surmy. AN Kasahskoy SSR Institut Metallurgii i Obogashcheniya. Available online: https://scholar.google.com/scholar?hl=en&as_sdt=0%2C5&q=Davlenye+Para+Trehsernistory+surmy+AC+Shendiyapin&btnG= (accessed on 1 June 2023).

23. Komorova, L.; HolmstrÖm, A.; Imris, I. Vaporization of Antimony from Synthetic Sulphosalts. *Scand. J. Metall.* **1985**, *14*, 103–112.

24. Habashi, F. Handbook of Extractive Metallurgy; Antimony; 1997; Volume 2. Available online: https://books.google.cl/books?id=wIpTAAAAMAAJ&redir_esc=y (accessed on 1 June 2023).

25. Zivkovic, Z.; Strbac, N.; Zivkovic, D.; Grujicic, D.; Boyanov, B. Kinetics and Mechanism of Sb2S3 Oxidation Process. *Elsevier Termochimica Acta* **2002**, *383*, 137–143. [CrossRef]

26. Steinhauser, J.; Vartiainen, A.; Wuth, W. Volatilization and Distribution of Impurities in Modern Pyrometallurgical Copper Processing from Complex Concentrates. *JOM* **1984**, *36*, 54–61. [CrossRef]

27. Davenport, W.G.; Jones, D.M.; King, M.J.; Partelpoeg, E.H. *Flash Smelting: Analysis, Control and Optimization*, 2nd ed.; Minerals, Metals & Materials Society: Pittsburgh, PA, USA, 2004.

28. Padilla, R.; Ramírez, G.; Ruiz, M.C. High-Temperature Volatilization Mechanism of Stibnite in Nitrogen-Oxygen Atmospheres. *Metall. Mater. Trans. B Process Metall. Mater. Process. Sci.* **2010**, *41*, 1284–1292. [CrossRef]

29. Qin, W.Q.; Luo, H.L.; Liu, W.; Zheng, Y.X.; Yang, K.; Han, J.W. Mechanism of Stibnite Volatilization at High Temperature. *J. Cent. South Univ.* **2015**, *22*, 868–873. [CrossRef]

30. Aracena, A.; Jerez, O.; Antonucci, C. Senarmontite Volatilization Kinetics in Nitrogen Atmosphere at Roasting/Melting Temperatures. *Trans. Nonferrous Met. Soc. China (Engl. Ed.)* **2016**, *26*, 294–300. [CrossRef]

31. Cabrera, E.; Aracena, A. *Encapsulamiento de Antimonio En Escoria Fayalítica Mediante Reducción Carbotérmica En Ambiente Neutro*; Pontificia Universidad Católica de Valparaíso: Valparaíso, Chile, 2018.

32. Kim, H.G.; Sohn, H.Y. Kinetic Modeling of Minor Element Behaviour in Copper Converting. In Proceedings of the Extraction and Processing Division, New Orlands, LA, USA, 17–21 February 1991.

33. Chaubal, P.C.; Sohn, H.Y.; George, D.B.; Bailey, L.K. Mathematical Modeling of Minor-Element Behavior in Flash Smelting of Copper Concentrates and Flash Converting of Copper Mattes. *Metall. Trans. B* **1989**, *20*, 39–51. [CrossRef]

34. Piacente, V.; Scardala, P.; Ferro, D. Study of the Vaporization Behaviour of Sb2S3 and Sb2Te3 from Their Vapour Pressure Measurements. *J. Alloys Compd.* **1992**, *178*, 101–115. [CrossRef]

35. Li, L.; Xu, M.; Li, Q. Arsenic Pre-Removal from Antimony Oxide Powder by Roasting with Pyrite (FeS2) for Decreasing Arsenic Transfer and Pollution in the Followed Antimony Smelting Process. *Sep. Sci. Technol.* **2022**, *57*, 1978–1991. [CrossRef]

36. Ouyang, Z.; Chen, Y.F.; Tian, S.Y.; Xiao, L.; Tang, C.B.; Hu, Y.J.; Xia, Z.M.; Chen, Y.M.; Ye, L.G. Thermodynamic and Kinetics Analysis of the Sulfur-Fixed Roasting of Antimony Sulfide Using ZnO as Sulfur-Fixing Agent. *J. Min. Metall. Sect. B Metall.* **2018**, *54*, 411–418. [CrossRef]

37. Haga, K.; Altansukh, B.; Shibayama, A. Volatilization of Arsenic and Antimony from Tennantite/Tetrahedrite Ore by a Roasting Process. *Mater. Trans.* **2018**, *59*, 1396–1403. [CrossRef]

38. Ye, L.; Wen, P.; Ouyang, Z.; Hu, Y.; Tang, C.; Xia, Z. Clean and SO2-Free Method for Bismuth Extraction from Bismuthinite by Multiphase Roasting: Thermodynamic Equilibria and Reaction Mechanisms. *JOM* **2020**, *72*, 3513–3520. [CrossRef]

39. Jin, W.; Yang, S.; Tang, C.; Li, Y.; Chang, C.; Chen, Y. Green and Short Smelting Process of Bismuth Sulphide Concentrate with Pyrite Cinder. *J. Clean. Prod.* **2022**, *377*, 134348. [CrossRef]

40. Jadhav, R.A.; Fan, L.S. Capture of Gas-Phase Arsenic Oxide by Lime: Kinetic and Mechanistic Studies. *Environ. Sci. Technol.* **2001**, *35*, 794–799. [CrossRef]

41. Zhang, W.; Che, J.; Xia, L.; Wen, P.; Chen, J.; Ma, B.; Wang, C. Efficient Removal and Recovery of Arsenic from Copper Smelting Flue Dust by a Roasting Method: Process Optimization, Phase Transformation and Mechanism Investigation. *J. Hazard. Mater.* **2021**, *412*, 125232. [CrossRef]

42. Tan, C.; Li, L.; Zhong, D.; Wang, H.; Li, K. Separation of Arsenic and Antimony from Dust with High Content of Arsenic by a Selective Sulfidation Roasting Process Using Sulfur. *Trans. Nonferrous Met. Soc. China* **2018**, *28*, 1027–1035. [CrossRef]

43. Liu, H.; Pan, W.-P.; Wang, C.; Zhang, Y. Volatilization of Arsenic During Coal Combustion Based on Isothermal Thermogravimetric Analysis at 600–1500 °C. *Energy Fuels* **2016**, *30*, 6790–6798. [CrossRef]

44. Aracena, A.; Ruiz, M.C.; Padilla, R. Oxidación de Enargita En Atmosferas de Nitrógeno-Oxígeno a Temperaturas Altas. *IBEROMET XI, X CONAMET/SAM* **2010**, *2*.

45. Nakazawa, S.; Yazawa, A.; Jorgensen, F.R.A. Simulation of the Removal of Arsenic during the Roasting of Copper Concentrate. *Metall. Mater. Trans. B* **1999**, *30*, 393–401. [CrossRef]

46. Fukuzawa, R.; Rao, S.R.; The Metallurgy and Materials Society Environment Section; Metals & Minerals Processing & the Environment in Memory of Dr. Ram Rao Symposium 2014.09.28-10.01 Vancouver, B.; Conference of Metallurgists 53 2014.09.28-10.01 Vancouver, B.; COM 53 2014.09.28-10.01 Vancouver, B. *Metals and Mineral Processing and the Environment in Memory of Dr. Ram Rao, Proceedings of the COM 2014, Conference of Metallurgists, 28 September–1 October 2014, Hyatt Regency Hotel, Vancouver, BC, Canada*; Canadian Inst. of Mining, Metallurgy and Petroleum: Vancouver, BC, Canada, 2014; ISBN 9781926872247.

47. Safarzadeh, M.S.; Howard, S.M.; Miller, J.D. Analysis and Visualization of Enargite and Tennantite Roasting Using Cu-As-S-O System Predominance Volume Diagrams. *Vacuum* **2018**, *156*, 78–90. [CrossRef]

48. Winkel, L.; Wochele, J.; Ludwig, C.; Alxneit, I.; Sturzenegger, M. Decomposition of Copper Concentrates at High-Temperatures: An Efficient Method to Remove Volatile Impurities. *Miner. Eng.* **2008**, *21*, 731–742. [CrossRef]

49. Bruckard, W.J.; Davey, K.J.; Jorgensen, F.R.A.; Wright, S.; Brew, D.R.M.; Haque, N.; Vance, E.R. Development and Evaluation of an Early Removal Process for the Beneficiation of Arsenic-Bearing Copper Ores. *Miner. Eng.* **2010**, *23*, 1167–1173. [CrossRef]

50. Yin, Z.; Lu, W.; Xiao, H. Arsenic Removal from Copper–Silver Ore by Roasting in Vacuum. *Vacuum* **2014**, *101*, 350–353. [CrossRef]

51. Padilla, R.; Chambi, L.C.; Ruiz, M.C. Antimony Production by Carbothermic Reduction of Stibnite in the Presence of Lime. *J. Min. Metall. Sect. B Metall.* **2014**, *50*, 5–13. [CrossRef]

52. Anderson, C.G. The Metallurgy of Antimony. *Geochemistry* **2012**, *72*, 3–8. [CrossRef]

53. Wang, Y.; Liu, C.; Zhu, X.; Ma, Z.; Li, L.; Zhang, L. Direct Preparation of Micro and Nano Antimony Trioxide Using Antimony Concentrate via Microwave Roasting: Mechanism and Process. *Ceram. Int.* **2022**, *48*, 23828–23839. [CrossRef]

54. Zhan, J.; Wang, Z.J.; Zhang, C.F.; Hwang, J.Y.; Xia, C.P. Separation and Extraction of Bismuth and Manganese from Roasted Low-Grade Bismuthinite and Pyrolusite: Thermodynamic Analysis and Sulfur Fixing. *JOM* **2015**, *67*, 1114–1122. [CrossRef]

55. Adham, K.; Harris, C. Two-stage fluid bed reactor for arsenic removal and fixation. In Proceedings of the Conference of Metallurgist (COM 2014), Canadian Institute of Mining, Metallurgy, and Petroleum, Vancouver, BC, Canada, 28 September–1 October 2014.

56. Yang, Y.B.; Cui, L.N.; Li, X.S.; Li, Q.; Jiang, T.; Ge, J. Novel Technology on Preparation of Double-Layered Pellets for Sulfur and Arsenic-Bearing Gold Concentrates. *J. Cent. South Univ.* **2013**, *20*, 2967–2973. [CrossRef]

57. Liu, S.; Su, Z.; Cai, Y.; Jiang, T.; Zhang, Y. An Efficient and Clean Method for the Selective Separation of Arsenic from Scrap Copper Anode Slime Containing High Arsenic and Tin. *J. Clean. Prod.* **2022**, *354*, 131640. [CrossRef]

58. Mihajlovic, I.; Strbac, N.; Zivkovic, Z.; Kovacevic, R.; Stehernik, M. A Potential Method for Arsenic Removal from Copper Concentrates. *Miner. Eng.* **2007**, *20*, 26–33. [CrossRef]

59. Lin, Y.; Hu, X.; Zi, F.; Chen, Y.; Chen, S.; Li, X.; Li, J.; Jiang, Y.; Zhang, Y. Rapid Gold Cyanidation from a Sulfur-High and Arsenic-High Micro-Fine Concentrate via Facile Two-Stage Roasting Pre-Treatment. *Miner. Eng.* **2022**, *190*, 107938. [CrossRef]

60. YAO, W.; MIN, X.; LI, Q.; LI, K.; WANG, Y.; WANG, Q.; LIU, H.; QU, S.; DONG, Z.; QU, C.; et al. Formation of Arsenic−copper-Containing Particles and Their Sulfation Decomposition Mechanism in Copper Smelting Flue Gas. *Trans. Nonferrous Met. Soc. China* **2021**, *31*, 2153–2164. [CrossRef]

61. HSC Chemistry [Software], Metso:Outotec 2023. Available online: https://www.metso.com/portfolio/hsc-chemistry/ (accessed on 23 June 2023).

62. Ouyang, Z.; Ye, L.; Tang, C.; Chen, Y. Phase and Morphology Transformations in Sulfur-Fixing and Reduction Roasting of Antimony Sulfide. *Metals* **2019**, *9*, 79. [CrossRef]

63. Li, Y.; Chen, Y.; Xue, H.; Tang, C.; Yang, S.; Tang, M. One-Step Extraction of Antimony in Low Temperature from Stibnite Concentrate Using Iron Oxide as Sulfur-Fixing Agent. *Metals* **2016**, *6*, 153. [CrossRef]

64. Liu, C.; Zhao, P.; Zhu, X.; Srinivasakannan, C.; Chen, M.; Zhang, M. A Novel Production Method of Antimony Trioxide from Stibnite Concentrate and the Dielectric Properties of Antimony Sulfide with Different Desulfurizer. *Miner. Eng.* **2021**, *171*, 107097. [CrossRef]

65. Li, Y.; Xue, H.; Taskinen, P.; Jokilaakso, A.; Tang, C.; Jin, W.; Rämä, M.; Chen, Y.; Yang, S. Clean Antimony Production from Stibnite Concentrate with Goethite Residue Co-Treatment for Zinc, Iron, Sulfur Conservation. *J. Clean. Prod.* **2021**, *313*, 127847. [CrossRef]

66. Li, Y.; Xue, H.; Taskinen, P.; Yang, S.; Tang, C.; Jin, W.; Chen, Y.; Jokilaakso, A. Sustainable Phase-Conversion Method for Antimony Extraction and Sulfur Conservation and Waste Treatment at Low Temperature. *J. Clean. Prod.* **2020**, *268*, 121950. [CrossRef]

67. Ye, L.; Tang, C.; Chen, Y.; Yang, S.; Yang, J.; Zhang, W. One-Step Extraction of Antimony from Low-Grade Stibnite in Sodium Carbonate—Sodium Chloride Binary Molten Salt. *J. Clean. Prod.* **2015**, *93*, 134–139. [CrossRef]

68. Lin, W.; Yang, S.; Tang, C.; Chen, Y.; Ye, L. One-Step Extraction of Bismuth from Bismuthinite in Sodium Carbonate–Sodium Chloride Molten Salt Using Ferric Oxide as Sulfur-Fixing Agent. *RSC Adv.* **2016**, *6*, 49717–49723. [CrossRef]

69. Chen, Y.; Zhu, S.; Taskinen, P.; Peng, N.; Peng, B.; Jokilaakso, A.; Liu, H.; Liang, Y.; Zhao, Z.; Wang, Z. Treatment of High-Arsenic Copper Smelting Flue Dust with High Copper Sulfate: Arsenic Separation by Low Temperature Roasting. *Miner Eng.* **2021**, *164*, 106796. [CrossRef]

70. Wu, G.; Wang, T.; Chen, G.; Shen, Z.; Pan, W.-P. Coal Fly Ash Activated by NaOH Roasting: Rare Earth Elements Recovery and Harmful Trace Elements Migration. *Fuel* **2022**, *324*, 124515. [CrossRef]

71. Song, B.; Song, M.; Chen, D.; Cao, Y.; Meng, F.; Wei, Y. Retention of Arsenic in Coal Combustion Flue Gas at High Temperature in the Presence of CaO. *Fuel* **2020**, *259*, 116249. [CrossRef]

72. Yang, K.; Qin, W.; Liu, W. Extraction of Metal Arsenic from Waste Sodium Arsenate by Roasting with Charcoal Powder. *Metals* **2018**, *8*, 542. [CrossRef]

73. Li, B.; Deng, J.; Jiang, W.; Zha, G.; Yang, B. Removal of Arsenic, Lead and Bismuth from Copper Anode Slime by a One-Step Sustainable Vacuum Carbothermal Reduction Process. *Sep. Purif. Technol.* **2022**, 123059. [CrossRef]

74. Shi, T.; He, J.; Zhu, R.; Yang, B.; Xu, B. Arsenic Removal from Arsenic–Containing Copper Dust by Vacuum Carbothermal Reduction–Vulcanization Roasting. *Vacuum* **2021**, *189*, 110213. [CrossRef]

75. Zhao, Z.; Wang, Z.; Xu, W.; Qin, W.; Lei, J.; Dong, Z.; Liang, Y. Arsenic Removal from Copper Slag Matrix by High Temperature Sulfide-Reduction-Volatilization. *J. Hazard. Mater.* **2021**, *415*, 125642. [CrossRef]